# Closeup exploration of the seafloor with an autonomous underwater helicopter

**Jing Zhou**
Zhejiang University
**Jiazhong He**
Zhejiang University
**Haocai Huang**
Zhejiang University
**Yingqiang Wang**
Zhejiang University
**Yulin Si**
Zhejiang University
**Shanhe Huang**
Zhejiang University
**Bo Xu**
Zhejiang University
**Ying Chen** ( zhoujing_zju@126.com )
Zhejiang University

**Research Article**

**Keywords:** seafloor exploration, marine science, underwater vehicles, autonomous underwater helicopter

**Posted Date:** May 28th, 2021

**DOI:** https://doi.org/10.21203/rs.3.rs-561628/v1

# Abstract

Closeup exploration of the seafloor requires new forms of underwater vehicles that are capable of taking off and landing on the seafloor and hovering at any attitude and that are equipped with cameras and sensors. Existing underwater vehicles do not provide an adequate platform for closeup in situ observations. This work presents the design, fabrication, control and testing of an autonomous underwater helicopter (AUH) that can perform spin turns, vertical rotation, free landing and take-off, making it the most agile underwater vehicle to date. Acoustic-optical navigation and gyroscopic stabilization systems were implemented to complete missions on a fixed route. With an underwater base station(helipad), the AUH can perform wireless power charging and data transmission. This work builds on previous generations of AUHs that were restricted to horizontal postures and lacked vectoring propulsion. Experimental results gathered from tests show that the AUH can successfully navigate along a preset route at depths ranging from 0 to 100 metres. Furthermore, with multidimensional attitude adjustment and vectoring propulsion, AUH is capable of diving into a rugged seafloor environment. This study advances what is currently achievable using traditional AUVs and ROVs, demonstrating methods that can be used in the future for studying marine science and seafloor exploration.


# Introduction

Until now, underwater exploration in marine biology and submarine resources has relied on underwater vehicles. Autonomous underwater vehicles (AUVs) and remote operated vehicles (ROVs) extend the range of human exploration, stepping into unknown regions that are otherwise unreachable.

Most underwater vehicles move in the water by thruster-based propulsion. AUVs are widely used because of their high speed and wide detection range[1]. They are able to analyse the environment autonomously by utilizing different sensors. However, AUVs mainly cruise in the upper ocean and can be easily trapped when approaching the seabed. Furthermore, it is difficult for an AUV to hover at a fixed point, which restricts its ability to make observations and perform operations at these locations. ROVs have strong and long-lasting operation capabilities and are currently the most effective and reliable underwater platforms for underwater operations. The ROV performs tasks under the guidance of a mother ship to which it must remain close, restricting its operation to within a certain range of the ship.

Submarine wheeled vehicles, i.e., crawlers, move directly on the seabed and have been widely applied in long-term monitoring[2, 3] and deep-sea sampling[4]. Unfortunately, crawlers do not perform well with sharp terrains; they may also modify the substrate on which they move[5]. Wheeled vehicles always have low gravity, which restricts their mobility[6]. The newly born category of underwater legged robots is a promising approach to ensure safe contact on uneven seabed, while maintaining agility and static stability.

Several underwater vehicles use bio-inspired structures and locomotion systems. Most biomimetic robots are built to mimic the morphology of an animal. Several prototypes that mimic fish[7–12], mantas[13–

15], octopi[16, 17] and crabs[18] have been created. The bio-inspired approach to the design of robots could potentially boost their adaptability and reduce noise, especially when interacting with the surrounding environment[19]. Most biomimetic underwater robots are slow speed systems as a result of their propulsion systems. Moreover, the space for payloads is fairly limited, and the operation capability is correspondingly weak.

Longevity and endurance are important challenges in the design of self-contained underwater robots. The expanding mission scope for underwater vehicles highlights the need for high-endurance operational capability, which is mainly dependent on the propulsion system efficiency and battery capacity of the vehicle. Increasing the energy storage capacity is an effective way to improve the mileage of underwater vehicles; however, this will result in an increase in the volume and power consumption of the device. The use of submerged docking stations permits battery recharge and data upload/download, which provides a method to elongate the endurance of underwater vehicles without compromising propulsion and payload power budgets[20–24]. Autonomous underwater docking is, however, complicated by the presence of currents and obstacles in the water and by the relative dynamic differences in orientation between the dock and the vehicle. A robust docking guidance system is therefore a core and crucial component for ensuring successful AUV docking.

There are abundant resources in the ocean, and the seafloor is an essential platform for geological prospecting and biological observation. However, the seafloor is not a boundless plain. The underwater terrain is rough with underwater mountains and valleys (Fig. 1). In situations with complicated terrain or navigation in narrow spaces, traditional underwater vehicles encounter large practical limitations. ROVs are, in essence, under-actuated systems, so its dirigibility is lacking, especially in complicated terrain. Umbilical cables connected to the deck control station further reduce the mobility of an ROV in a restricted space. AUV mobility is not restricted by umbilical cables; however, its torpedo shape and under-actuation characteristics make it easily trapped near the sea bottom. Existing underwater vehicle prototypes do not provide an adequate platform for closeup observations of the seafloor.

We sought to build and successfully deploy an underwater vehicle that can autonomously cruise close to the seabed. The challenges mainly lie in three aspects: (i) the AUH has to adjust its attitude and direction in an ultraflexible way to explore the rugged and varied seabed environment; (ii) to avoid emerging from under the sea too frequently, the AUH has to perform power charging and data transmission in the lower ocean; and (iii) the AUH has to be able to navigate in a weak communication environment and complete accurate docking.

A new form of seafloor-resident underwater vehicle is proposed in this paper, the autonomous underwater helicopter (AUH), which is capable of taking off and landing on the seafloor and hovering at any attitude. It can be equipped with cameras and sensors for scientific surveys. In addition, the AUH works collaboratively with underwater helipads. When docking with the helipad, the AUH performs wireless power charging and data transmission before starting a new cruising task. As a result of the support from the helipad, the AUH can endure the conditions in the lower ocean for a long time.

Building on the experience of S-AUH, G-AUH, ICE-AUH and CORAL-AUH[25–35], we developed an ultramobile AUH with advanced propulsion, navigation and wireless charging systems. We demonstrate advantages of the ultramobile AUH in real-world scenarios (reported data were taken from 6 missions at different time in swimming pool/pond/real sea conditions). We believe that AUHs have the potential for greater manoeuvrability than other underwater devices, which could ensure their longevity in deep oceans for large-scale continuous observations.

# Results

Inspired by the bottom-dwelling stingray, we developed a disk-shaped AUH as a seafloor-resident underwater vehicle(See Fig. 2). The AUH measures 0.94 m × 0.94 m × 0.28 m, weighs 15 kg, is neutrally buoyant, and can swim for 30 min at a time. The AUH has an attitude adjustment system and vectoring propulsion system, which enables it to adjust to the desired attitude before propelling forward or backward. An acoustic transducer and camera are mounted on the bottom of the AUH to receive acoustic and optical signals, respectively.

### Ultramobility

The ultramobility of the AUH is achieved via an attitude adjustment system and vectoring propulsion system. The attitude adjustment system assembly is composed of two turn plates, with buoyancy material cubes and interlaced leads distributed throughout. Each propeller is mounted on a steering motor to change the direction of the propulsion.

The AUH adjusts the relative angle of two turn plates to achieve a range of attitudes and performs. left and right turns through the differential speed control of opposite propellers. The AUH can perform deflections in any direction, with a maximum baseline deflection of ± 90°. Similarly, the AUH can pitch its dive planes in any direction, with a maximum pitch of ± 90°. A sample AUH trajectory is shown in Fig. 3, illustrating the ultra-agile swimming motion following preset commands. The AUH can change attitude, direction and depth while exploring the seafloor, with an average swimming speed of 1.28 m/s (± 0.26 m/s) at depths of 0 to 100 m.

We performed quantitative tests in a pool to measure the propulsion and attitude adjustment capabilities of the AUH. The average swimming speed in a straight path was 1.54 m/s (± 0.06 m/s), equivalent to 1.5 body lengths per second. The average angular spin rate was 3.14 rad/s (± 0.6 rad/s) with a zero turning radius. Vertical diving can be achieved either in the vertical or horizontal attitude. The average dive speed in the vertical attitude is 1.22 m/s (± 0.08 m/s), equivalent to 1.2 body lengths per second. The average dive speed in the horizontal attitude is 0.72 m/s (± 0.07 m/s), equivalent to 0.7 body lengths per second. Diving in the vertical attitude is ideal for gross depth changes, while diving in the horizontal attitude is suitable for fine depth adjustments.

### Navigation and motion actuators

The navigation system of the AUH consists of an inertial measurement unit (IMU), an inverse ultra-short baseline (I-USBL) system and depth sensor (Fig. 4). I-USBL is a new system for underwater acoustic positioning(56). Normally, the transmitter of the USBL is placed on the underwater vehicle, and multiple receiving unit arrays are placed on the ship/shore base station. After receiving signals sent from the underwater vehicle, the ship/shore base station determines the location and attitude information. Acoustic communication is necessary for the underwater vehicle to acquire its own position. This paper presents an inverse ultra-short baseline system in which a six-element receiving array on the AUH and one transmitter on the base station are used. In this case, the acoustic communication equipment can be omitted.

The motion actuators in AUH include the gear-side motor, steering motor and propeller. The motion control panel perceives data from sensors, and output motion commands after position calculation. The inertial measurement unit (IMU) measures the three-axis attitude angle and acceleration rate of the AUH. The inverse ultra-short baseline (I-USBL) system is used to determine the exact position of the AUH according to the delay difference in the acoustic signals sent to and received from the vehicle. The depth sensor measures the depth of the AUH. Having received data from the positioning system, the motion control panel then calculates the actual position of the AUH and compares it with the target position and sends commands to the attitude adjustment system and propulsion system accordingly.

### Underwater helipad

The underwater helipad is the home base of the AUH; it provides docking and protection for the AUH and connects to the shore base station via a photoelectric composite cable. The helipad is made of steel pipe frames and is equipped with an acoustic transducer, guiding light, camera and wireless charging system. In the whole docking process, a main control module is responsible for the coordination and operation of each functional unit. The docking process is described as follows. First, the acoustic communication unit on the helipad obtains position information for the AUH and perceives its working state. When the AUH approaches the helipad, the AUH switches to visual navigation mode, and the guiding light is turned on to help the AUH dock with the helipad. After the AUH successfully docks, the wireless charging unit is activated, and the AUH obtains energy from the helipad in a contact-less way.

Wireless power transfer involves inherent electrical isolation between the primary and secondary sides, which ensures safe charging in an underwater environment. This breakthrough technology greatly facilitates deep-sea power transmission. The wireless power and data transmission capability of the system were tested in a pool. The resonant system operates at 35.4 kHz at a depth of 2 m, and the wireless power transmission distance is 20 mm. An individual transmission path for simultaneous data transfer was built with a Wifi module. The data upload and download rate is approximately 1000 bits/s at a 20 cm distance. The results indicate that more than 98% of the data were successfully received. The docking experiment was carried out in a swimming pool and a pond separately. In the pond, the AUH docked successfully to the helipad 9 out of 10 times, while in the swimming pool, the docking success rate was 100%.

# Discussion

We have presented a novel seafloor-resident underwater vehicle, an autonomous underwater helicopter (AUH), that demonstrated prolonged and consistent seafloor-resident capability. Whereas most autonomous underwater vehicles cruise and operate in the upper ocean, our underwater helicopter features ultramobility and seafloor-resident capability for seafloor tasks. The acoustic-optic navigation system provides a compact, software-defined modulation scheme for docking with the helipad that is robust to noise and interference from a complex environment.

We demonstrated that the AUH can work in indoor environments and open seas. The next steps are test AUH in severe environments(with greater flows and depth), to use the AUH as an instrument to (i) study the behaviour of marine life on the seafloor and (ii) explore seabed resources, and to create AUH swarms across different scales.

# Methods

### System architecture

The AUH system and main sub-components are shown in Fig. 1. The electronics module includes a waterproof housing for the camera, microcomputer, main control chip, motor driver, battery, inertial navigation and gyroscopic stabilization system. The housing is composed of two acrylic domes surrounding an aluminium ring and waterproofed with an O ring(passed 100m pressure test). Inlet wire channels are inserted on the side face of the acrylic ring. Outside the electronics module is the attitude adjustment system assembly, consisting of two turn plates with buoyancy material (white) and leads (black) fixed to them. Four equally-spaced vectoring propellers are mounted to the outer turn plate. The vectoring propeller assembly is composed of a steering motor and a propeller. The system is covered by a 3D-printed shell, the shape of which is hydrodynamically optimized. Two fluid channels (horizontal and vertical) are preset on the shell for each vectoring propeller.

### Attitude adjustment

The attitude adjustment system assembly includes two turn plates that can rotate freely on ball bearings. Two buoyancy material cubes and leads are fixed to each turn plate. By rotating the turn plates, the centre of gravity and centre of buoyancy can be changed, and the attitude of the AUH can be adjusted (Fig. 5): (i) At the initial position, the buoyancy cubes and leads are aligned in a staggered manner, and the AUH is in a horizontal attitude. (ii) The inner turn plate rotates 180 degrees relative to the initial position;, the centre of gravity is on one side of the AUH, while the centre of buoyancy is on the other side, and the posture of the AUH becomes vertical. (iii) The inner turn plate rotates 90 degrees relative to the initial position, and the posture of AUH becomes vertical. The propulsion direction of the vectoring propeller is 45 degrees.

### Vectoring propulsion

Four vectoring propellers are equidistantly arranged on the outer ring of the AUH. Integrating posture adjustment with vectoring propulsion, the AUH is capable of accomplishing three-dimensional movement with a zero turning radius, making it the most agile underwater vehicle. 1) Horizontal movement. The AUH adjusts to a horizontal posture, and two opposite propellers propel forward and backward at the same speed. 2) Vertical movement. For large-scale vertical movement, the AUH adjusts to a vertical posture, and two opposite propellers propel forward and backward at the same speed. For fine-tuned movement, the AUH adjusts to a horizontal posture, and the four propellers propel forward and backward at the same speed. 3) Oblique movement. The AUH adjusts to an oblique posture, and two opposite propellers propel forward and backward at the same speed. 4) Steering. Two opposite propellers propel the AUH forward and backward at different speeds. 5) Spin turn. Two opposite propellers propel in reverse directions.

## Acoustic positioning

The positioning system of the AUH consists of an inertial measurement unit (IMU), an inverse ultra-short baseline (I-USBL) system and depth a sensor (Fig. 6). I-USBL is a new system for underwater acoustic positioning. Normally, the transmitter of the USBL is placed on the underwater vehicle, and multiple receiving unit arrays are placed on the ship/shore base station. After receiving signals sent from the underwater vehicle, the ship/shore base station determines the location and attitude information. Additional acoustic communication is compulsory for the underwater vehicle to acquire its own position. This paper presents an inverse ultra-short baseline system in which a six-element receiving array on the AUH and one transmitter on the base station (the helipad) are used. The AUH vehicle can obtain positioning information directly from the receiver module rather than waiting for conventional USBL results transmitted from the acoustic modem on the surface vessel. Provided accurate clock synchronization on both the transmitter and receiver, the AUH could range itself once the transmitted signal arrives while being acoustically passive. In this case, the acoustic communication equipment can be omitted, and the passive receiver array on the AUH would consume much less energy.

The acoustic transmitter is housed in the underwater helipad, which incorporates an embedded processor, a power amplifier and a synchronized clock into an aluminium cylindrical waterproof cabin (ϕ202 mm*352 mm). The pre-designed signal is generated by a digital signal processor (DSP, TMS320C6748 from Texas Instruments) and transmitted through a field programmable gate array (FPGA, Spartan 6 from Xilinx) triggered by the rising edge of a synchronous PPS clock. We chose a 200-Watt class-D power amplifier placed ahead of the spherical omnidirectional underwater speaker to ensure a reasonable effective propagation zone. The pulse-per-second (PPS) signal of the synchronous clock is pre-calibrated using a GPS antenna above the water and kept synchronized underwater utilizing a chip-scale atomic clock (CSAC)(35).

The acoustic receiver consists of a six-element circular hydrophone array(57,58), a front-end amplifier and an embedded processor that incorporates a DSP and FPGA. In contrast to the transmitter scenario, the hydrophones of the receiver convert the arrived acoustic signal to a measurable electrical analogue signal; subsequently, the front-end amplifier delivers a voltage-level signal to a high-speed analogue-to-

digital converter (AD7606) for sampling. The FPGA continuously keeps sampling triggered by the receiver PPS clock synchronized to that on the transmitter.

The transmitted signal is a pre-recorded 10 ms, 8–14 kHz linear up-chirp in consideration of the propagation distance and auto-correlation coefficient. The transmitter and receiver transmit and receiver signals at the same moment, which is the rising edge of the PPS. There is a meaningful time delay in the received signal standing for time of flight (TOF) that can be determined by a correlation process using known signal characteristics in both the time and frequency domains. Provided accurate conductivity, temperature and depth, the sound velocity can be determined and used to range the distance between the transmitter and receiver.

Azimuth is an essential parameter in underwater localization in addition to the distance mentioned above. To precisely estimate the azimuth, we set a horizontal circular 6-element array with hydrophones uniformly spaced in a diameter of 130 millimetre, whose geometry suits our disc-shaped AUH well. Beamforming is widely used for azimuth estimation. We use the deconvolved conventional beamforming (dCv) algorithm, which can achieve a narrow beam width with low sidelobes, providing a high directivity factor (DF).

### Optical guided docking

In the far end, the AUH determines its position with an acoustic transducer and navigates towards the helipad. On approaching the helipad, the AUH gradually adjusts its posture to align with the target orientation. In the near end, the AUH tracks the navigation lights with a machine vision algorithm to adjust its position and posture precisely and dock with the helipad successfully.

When the distance between the AUH and helipad is within a given value, the AUH switches to visual navigation mode. The camera will first detect whether the light source is within the camera view. If the light source is not found, the AUH will keep moving to obtain a large field of view for a second detection. If the second detection fails, the AUH determines that the helipad is still at a distance away will switch back to acoustic navigation mode until the light source is finally detected.

Once the light source is detected, a program written in Python will call the camera to capture an image frame. Image pre-processing is conducted afterwards, including de-interference, noise reduction, sharpening, de-distortion and binarization.

According to the image processing algorithm, the features of the image are extracted and analysed to obtain the relative deviation angle and pixel distance between the AUH and the helipad. These processing results are sent to the STM32 through the serial port. The propellers are modulated according to the calculated deviation angle and distance through closed-loop PID control. Once the docking conditions are met, the propellers adjust the AUH to vertical attitude and push the vehicle downwards into the helipad(See Fig. 7).

### Underwater Helipad

The helipad is the home port of the AUH. The supporting frame of the helipad is made of 980 steel pipes, 2.5 m in length and width, and 1.2 m in height. The main external frame of the support is the main bearing structure; it is welded with steel pipe with an outer diameter of 50 mm and a wall thickness of 5 mm. The internal supporting steel pipe is a square pipe with a wall thickness of 5 mm and a diameter of 50 mm. The helipad is a truss-like structure that fully utilizes its material strength with a minimal main frame weight. The helipad is small on the top and large at the bottom, which increases its standing stability. Its upper end is equipped with a guiding light and an acoustic transducer, and the lower end is equipped with mounting brackets, an electronic control cabin, a standby power supply cabin, and an underwater camera. The cabins are made of 6061 aluminium alloy. When the AUH docks with the helipad, the lander lands on a porous mounting plate.

After the AUH docks with the helipad, a locking device is activated, and wireless charging starts. Meanwhile, cruising data is uploaded, and a new task is downloaded to the AUH. A compact wireless power transfer system was built to enable contact-less power transmission from the helipad to the AUH. The WPT system, consisting of a DC voltage source, H-bridge inverter, magnetic coupler, compensation network, rectifier, capacitive filter, and controllers, is separated into two isolated parts, i.e., the primary side and the secondary side, as shown in Fig. 8. On the primary side, the H-bridge inverter outputs high frequency AC current to the primary side coil, establishing a high-frequency magnetic field. The high-frequency magnetic field is transferred to the secondary side coil through magnetic coupling, and then the secondary side rectifier converts the AC voltage to DC voltage, which is finally used to charge the battery with constant current output. As the equivalent resistance of the battery varies throughout the charging process, the WPT system should be able to maintain a constant output current and constant input current phase to retain stable and efficient operation. An LCCL compensation topology enables the system to output a constant current throughout the charging process.

A mechanical guidance frame ensures alignment of the transmitter and receiver coils. The electromagnetic coupling structure is shown in Fig. 8. As the acoustic receiver array is placed at the bottom of the AUH, the receiver coil is placed a distance away to reduce electromagnetic interference and increase efficiency.

## Open-sea experiments

We tested the ultra-mobility of AUH in the open ocean, in which AUH takes typical actions like spin, vertical rotary, vectoring propulsion and hovering at any attitude in a complex underwater environment. Three dives were conducted over the course of 2 days, exploring in the Luhuitou Bay in Sanya, China. This environment offers complicated seabed topography with varying tidal conditions, allowing AUH to be evaluated in real-world conditions.

The AUH conducted about 30 min of continuous motion during each dive, at an average depth of 8 m and a maximum depth of 12 m. All of these tests evaluated the effectiveness of the AUH in ultra mobile motion control. The AUH’s trajectories were recorded by two divers using GoPro from distance of several metres.

# Declarations

### Author contributions statement

Jing Zhou, Jiazhong He designed the AUH, Yingqiang Wang and Shanhe Huang developed the acoustic navigation system. Bo Xu and Yulin Si designed the helipad and docking algorithm. Jiazhong He and Bo Xu conducted the experiments, Haocai Huang and Ying Chen analysed the results. All authors reviewed the manuscript.

# References


1. R. Wynn, V. Huvenne, T. Le Bas, B. Murton, D. Connelly, B. Bett, H. Ruhl, K. Morris, J. Peakall, D. Parsons, Autonomous Underwater Vehicles (AUVs): Their past, present and future contributions to the advancement of marine geoscience. *Marine Geology*. **SI 352**: 451-468 (2014)
2. C. Doya, D. Chatzievangelou, N. Bahamon, A. Purser, F. C. De Leo, S. K. Juniper, L. Thomsen, J. Aguzzi, Seasonal monitoring of deep-sea megabenthos in Barkley Canyon cold seep by internet operated vehicle (IOV). *PLOS ONE* **12**, e0176917 (2017).
3. Laschi, B. Mazzolai, M. Cianchetti, Soft robotics: Technologies and systems pushing the boundaries of robot abilities. *Sci. Robot.* **1**, 1–12 (2016).
4. Yoshida, T. Aoki, H. Osawa, S. Ishibashi, Y. Watanabe, J. Tahara, T. Miyazaki, K. Itoh, A deepest depth ROV for sediment sampling and its sea trial result, in *2007 Symposium on Underwater Technology and Workshop on Scientific Use of Submarine Cables and Related Technologies* (IEEE, 2007), pp. 28–33.
5. Wang, X. Yang, Y. Chen, D. K. Wainwright, C. P. Kenaley, Z. Gong, Z. Liu, H. Liu, J. Guan, T. Wang, J. C. Weaver, R. J. Wood, L. Wen, A biorobotic adhesive disc for underwater hitchhiking inspired by the remora suckerfish. *Sci. Robot*. **2**, eaan8072 (2017).
6. Inoue, T. Shiosawa, K. Takagi, Dynamic analysis of motion of crawler-type remotely operated vehicles. *IEEE J. Ocean. Engi*. **38**, 375–382 (2013).
7. Wang, X. Yang, Y. Chen, D. K. Wainwright, C. P. Kenaley, Z. Gong, Z. Liu, H. Liu, J. Guan, T. Wang, J. C. Weaver, R. J. Wood, L. Wen, A biorobotic adhesive disc for underwater hitchhiking inspired by the remora suckerfish. *Sci. Robot.* **2**, eaan8072 (2017).
8. S. Marras, M. Porfiri, Fish and robots swimming together: Attraction towards the robot demands biomimetic locomotion. *J. R. Soc. Interface* **9**, 1856–1868 (2012).
9. A. D. Marchese, C. D. Onal, D. Rus, Autonomous soft robotic fish capable of escape maneuvers using fluidic elastomer actuators. *Soft Robot.* **1**, 75–87 (2014).
10. R. K. Katzschmann, A. D. Marchese, D. Rus, Hydraulic autonomous soft robotic fish for 3D swimming, in *Experimental Robotics: The 14th International Symposium on Experimental Robotics, M. A. Hsieh, O. Khatib, V. Kumar, Eds.* (Springer International Publishing, 2014), vol. 109, pp. 405–420.

11. A. D. Marchese, C. D. Onal, D. Rus, Towards a self-contained soft robotic fish: On-board pressure generation and embedded electro-permanent magnet valves, in *Experimental Robotics: The 13th International Symposium on Experimental Robotics, J. P. Desai, G. Dudek, O. Khatib, V. Kumar, Eds.* (Springer International Publishing, 2013), vol. 88 of Springer Tracts in Advanced Robotics, pp. 41–54.
12. P. Phamduy, M. Vazquez, A. Rizzo, M. Porfiri, Miniature underwater robotic fish for animal-robot interactions, in *ASME 2016 Dynamic Systems and Control Conference* (ASME, 2016), vol. 2, p. V002T17A009.
13. K. Suzumori, S. Endo, T. Kanda, N. Kato, H. Suzuki, A bending pneumatic rubber actuator realizing soft-bodied manta swimming robot, in *International Conference on Robotics and Automation* (IEEE, 2007), pp. 4975–4980.
14. A. Cloitre, B. Arensen, N. M. Patrikalakis, K. Youcef-Toumi, P. V. Y. Alvarado, Propulsive performance of an underwater soft biomimetic batoid robot, in *The Twenty-fourth International Ocean and Polar Engineering Conference* (International Society of Offshore and Polar Engineers, 2014), vol. 3, pp. 326–333.
15. T. Li, G. Li, Y. Liang, T. Cheng, J. Dai, X. Yang, B. Liu, Z. Zeng, Z. Huang, Y. Luo, T. Xie,
16. Yang, Fast-moving soft electronic fish. *Sci. Adv.* **3**, e1602045 (2017).
17. M. Calisti, M. Giorelli, G. Levy, B. Mazzolai, B. Hochner, C. Laschi, P. Dario, An octopus bioinspired solution to movement and manipulation for soft robots. *Bioinspir. Biomim.* **6**, 036002 (2011).
18. F. G. Serchi, A. Arienti, I. Baldoli, C. Laschi, An elastic pulsed-jet thruster for Soft Unmanned Underwater Vehicles, in *2013 IEEE International Conference on Robotics and Automation (ICRA)* (IEEE, 2013), pp. 5103–5110.
19. G. Picardi, M. Chellapurath, S. Lacoponi, S. Stefanni, C. Laschi, M. Calisti, Bioinspired underwater legged robot for seabed exploration with low environmental disturbance. *Sci. Robot.* **5**, eaaz1012 (2020)
20. R. K. Katzschmann, J. DelPreto, R. MacCurdy, D. Rus, Exploration of underwater life with an acoustically controlled soft robotic fish. *Sci. Robot.* **3**, eaar3449 (2018).
21. H. Singh, J. G. Bellingham, F. Hover, S. Lemer, B. A. Moran, K. von der Heydt, D. Yoerger, Docking for an autonomous ocean sampling network. *IEEE J. Oceanic Engi.*, **26**(4), 489-514(2001).
22. T. Kawasaki, T. Fukasawa, T. Noguchi, M. Noguchi, Development of AUV "Marine Bird" with underwater docking and recharging system, in *Proceedings of the 3rd International Work-shop on Scientific Use of Submarine Cables and Related Technologies* (IEEE, 2003), pp. 166-170.
23. J. G. Shi, D. J. Li, C. J. Yang, Design and analysis of an underwater inductive coupling power transfer system for autonomous underwater vehicle docking applications. *J. Zhejiang Uni.-Sci. C* **15**(1), 51-62 (2014).
24. T. Zhang, D. J. Li, C. J. Yang, Study on impact process of AUV underwater docking with a cone-shaped dock. *Ocean Engi.* **130**, 176-187 (2017).
25. R. Zheng, T. Song, Q. G. Sun, J. Q. Guo. Review on underwater docking technology of AUV. *Chinese J. Ship Research* **13**(6): 43-49, 65 (2018).

26. C. W. Chen, Y. Jiang, H. C. Huang, D. X. Ji, G. Q. Sun, Z. Yu, Y. Chen, Computational Fluid Dynamics Study of the Motion Stability of an Autonomous Underwater Helicopter. Ocean Engi. 143, 227-239 (2017).
27. Z. Feng, C. Chen, Z. Yu, H. Huang, H. Su, J. Leng, Y. Chen, Hydrodynamic performance analysis of underwater helicopter based on STAR-CCM, in OCEANS-MTS (IEEE, 2018).
28. Q. Cai, C. Chen, Z. Yu, H. Huang, N. Yan, H. Su, J. Leng, Y. Chen, Numerical Analysis of Hydrodynamic Interaction for AUH and Mother Ship in Different Regular Wave Directions, in OCEANS-MTS (IEEE, 2018).
29. C. Chen, N. Yan, Prediction of added mass for an autonomous underwater vehicle moving near sea bottom using panel method. in 4th International Conference on Information Science and Control Engineering (ICISCE 2017), pp.1094-1098.
30. C. Chen, N. Yan, J. Leng, Y. Chen, Numerical analysis of second-order wave forces acting on an autonomous underwater helicopter using panel method, in OCEANS-MTS (IEEE 2017).
31. C. Chen, Y. Jiang, C. Huang, J. Leng, Z. Yu, H. Su, Y. Chen, Computational fluid dynamics study on magnus force of an autonomous underwater helicopter, in OCEANS-MTS (IEEE 2017).
32. C. Chen, C. Huang, X. Dai, H. Huang, Y. Chen, Motion and control simulation of a dished autonomous underwater helicopter. in OCEANS-MTS (IEEE 2017).
33. Z. Wang, X. Liu, H. Huang, Y. Chen, Development of an underwater autonomous helicopter with high maneuverability, Appl. Sci. 9(19), 2671 (2019).
34. D. Ji, C. Chen, Y. Chen, Autonomous Underwater Helicopters, AUV with Disc-shaped Design for Deepwater Agility. Sea Tech., Jan. 2018
35. X. Liu, Z. Wang, Y. Guo, Y. Wu, G. Wu, H. Huang, Y. Chen, The Design of Control System based on Autonoumous Underwater Helicopter. in OCEANS-MTS (IEEE 2018)
36. C. Chen, T. Wang, Z. Tong, Y. Lu, H. Huang, D. Ji, Y. Chen, Simulation research on water entry impact force of an autonomous underwater helicopter. J. Marine Sci. and Tech. (2020). DOI 10.1007/s00773-020-00707-8

# Figures

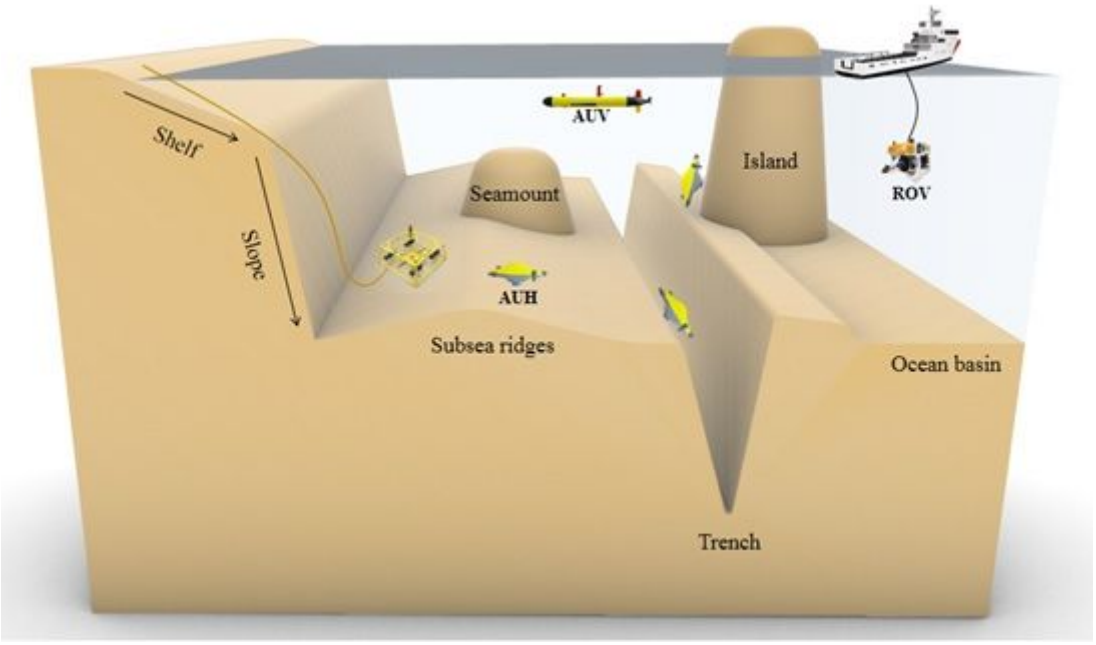


## Figure 1

Ocean topography and underwater vehicles. AUVs cruise in the upper ocean. ROVs operate in a single location with a ship as the base. AUHs feature ultramobility and seafloor-resident capability in seafloor tasks.

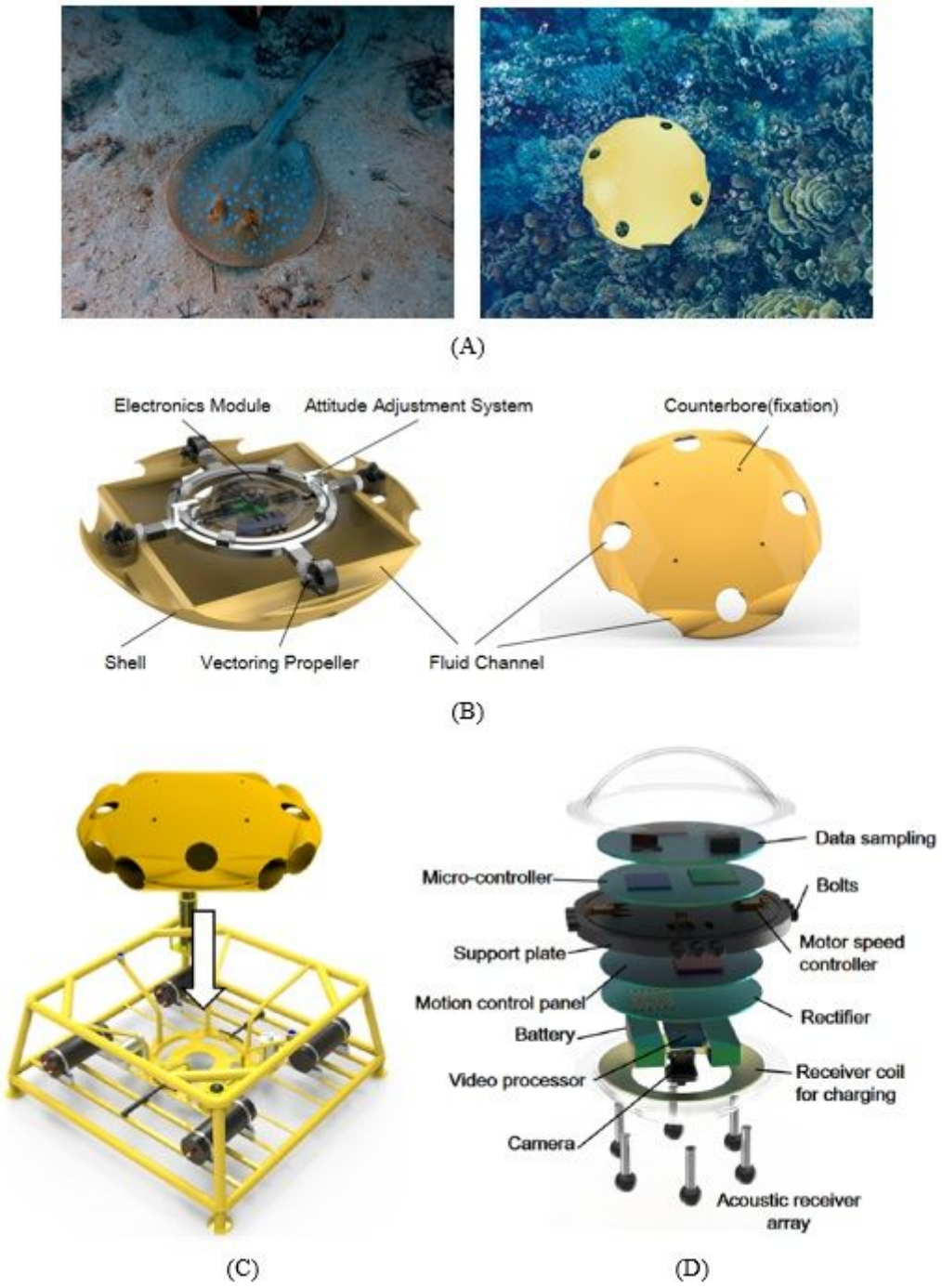


## Figure 2

AUH system overview. (A) The shape of AUH was inspired by a stingray. (B) Components of the AUH. (C)AUH docked into the helipad for wireless power charging and data transmission. (D) Exploded view of the electronic cabin.

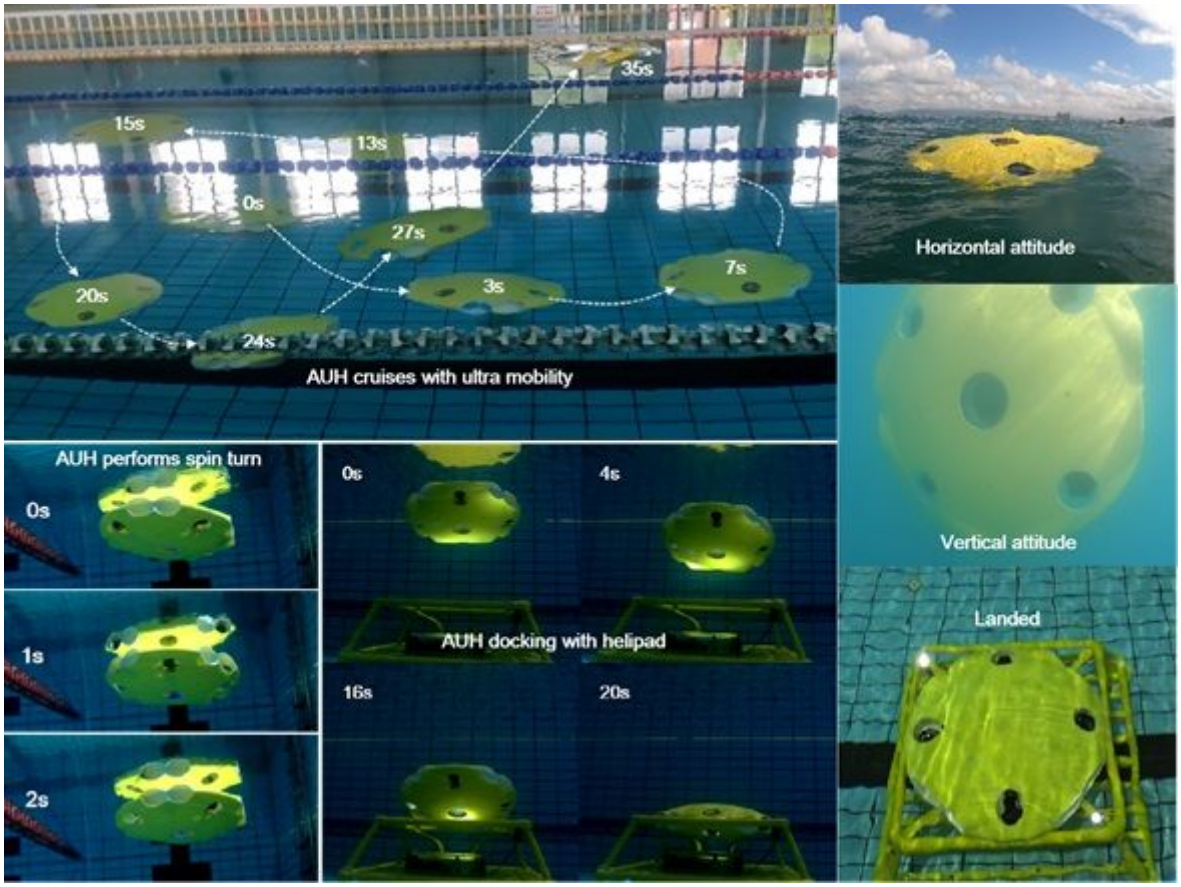


## Figure 3

Sample AUH trajectory. (Top) The AUH cruises with ultra mobility. (Bottom left) The AUH makes a spin turn. (Bottom middle) The AUH docking into the helipad. (Right) AUH in multiple states.

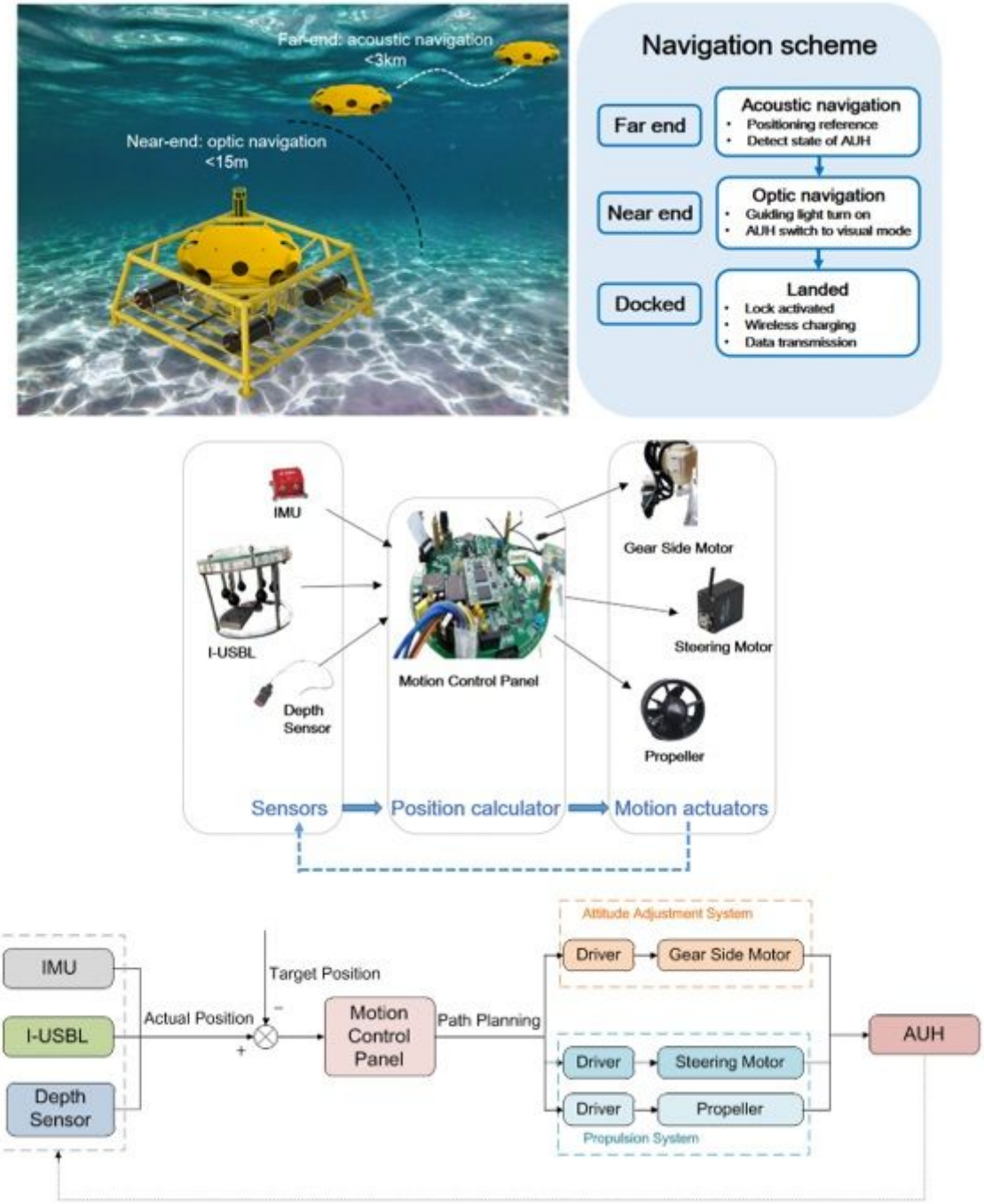


## Figure 4

Flow chart of the navigation and actuation system. (Top) Acoustic-optic navigation scheme. (Middle) Components of acoustic navigation and actuation system. (Bottom) Control scheme in acoustic navigation mode.

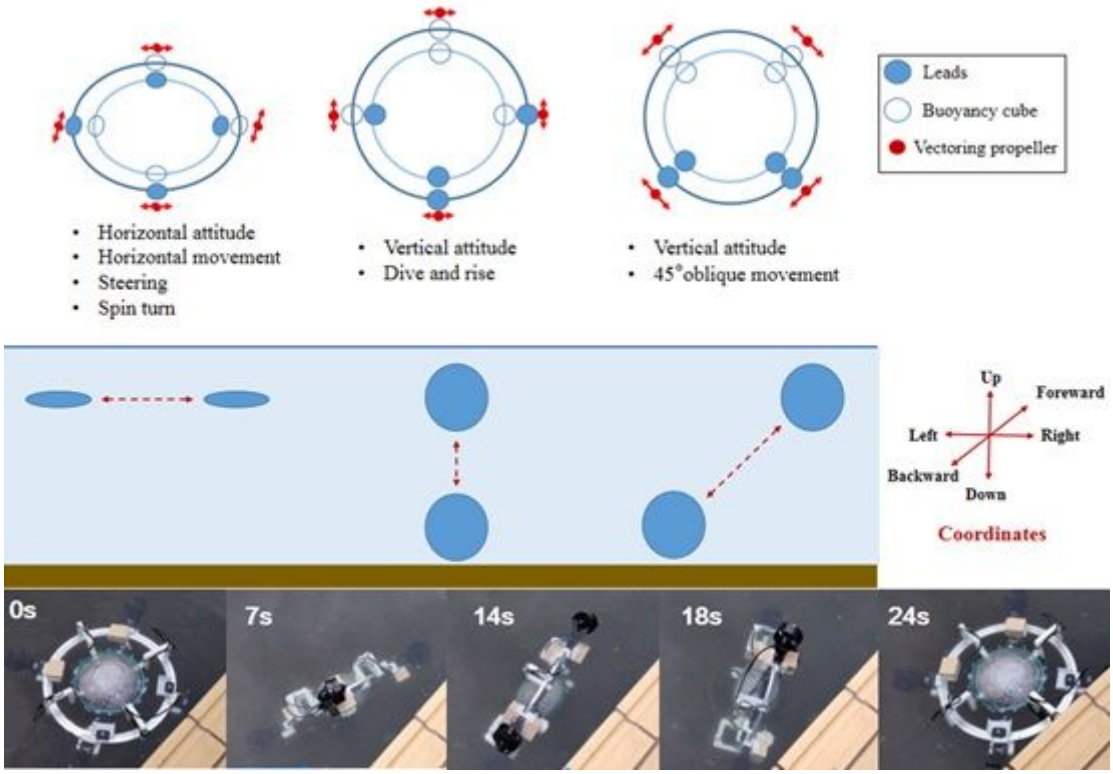


## Figure 5

Multidimensional attitude adjustment. (Top) Different alignments of buoyancy cubes and leads result in various postures and movement directions, and diagrammatic sketch of movement in the sea and corresponding coordinates. (Bottom) Attitude adjustment of the AUH.

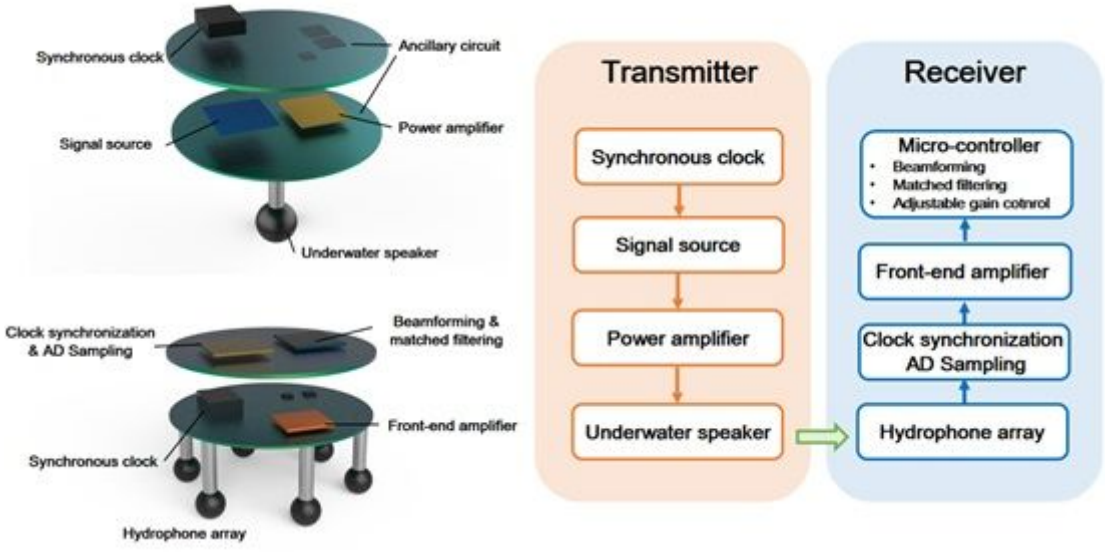


## Figure 6

Acoustic positioning system. (Left) Exploded view of the acoustic transmitter and receiver array. (Right) Flow chart of the acoustic positioning system.

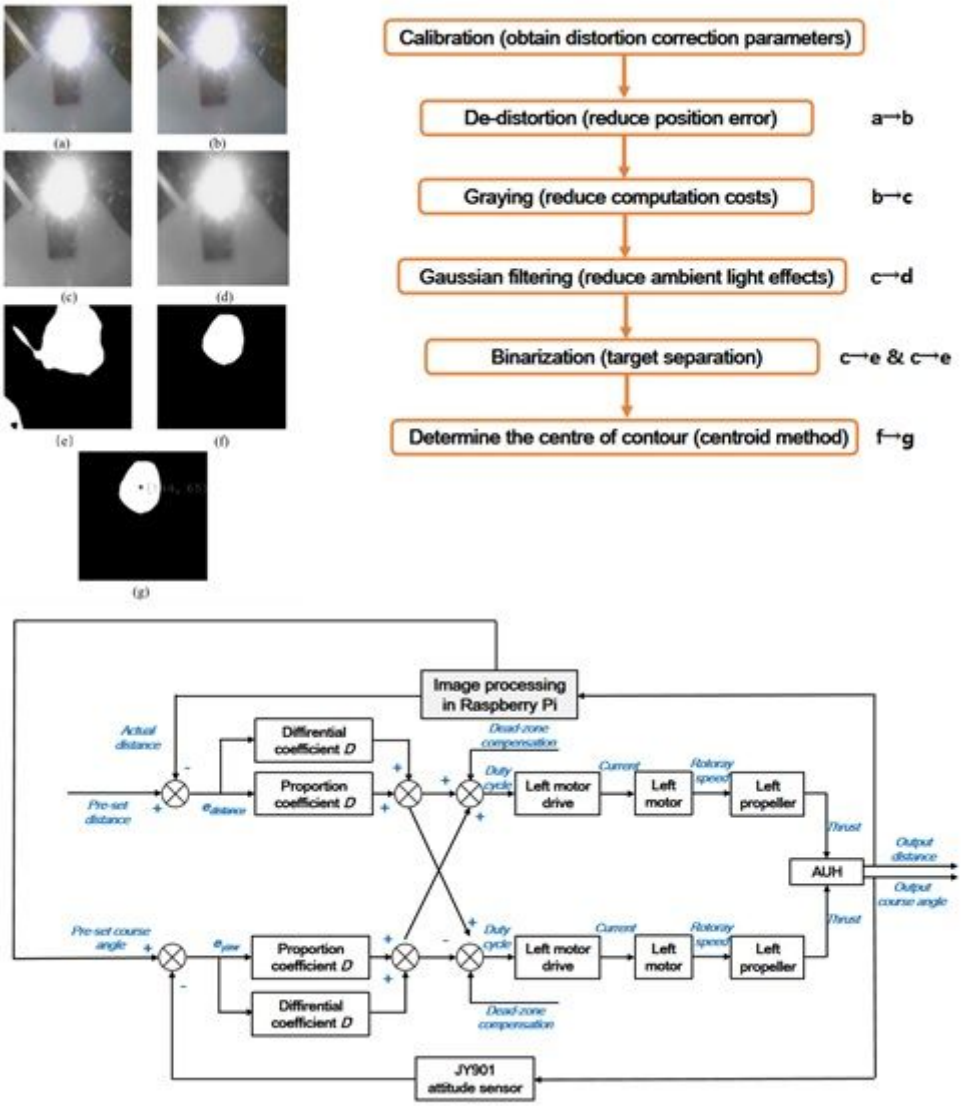


## Figure 7

Optical guided docking system. (Top) Image processing procedures in Raspberry Pi. (Bottom) PID control of motion during docking.

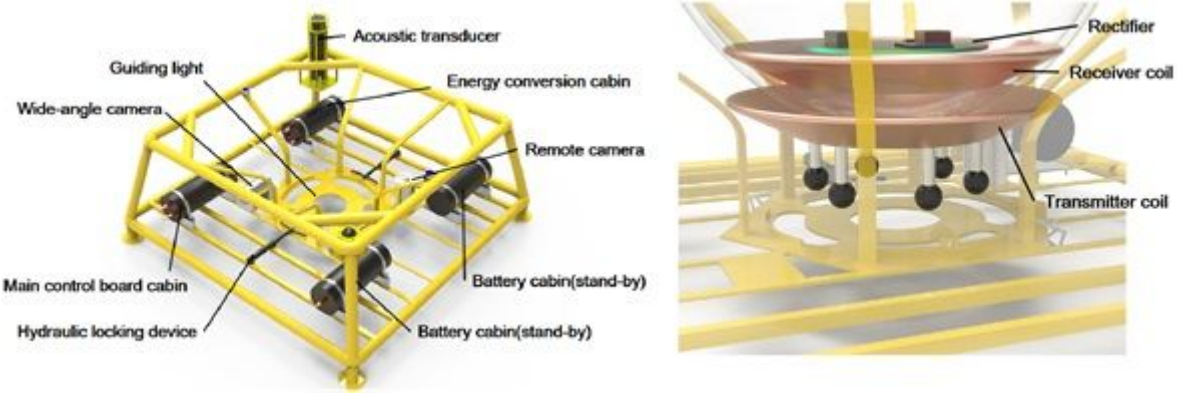


## Figure 8

Underwater helipad. (Left) Components in the underwater helipad. (Right) In the wireless power transfer system, the transmitter coil is attached to the helipad, the receiver coil is located inside the electronic cabin of AUH.